

# Microtubule Acetylation Promotes Kinesin-1 Binding and Transport

Nathan A. Reed,<sup>1,3</sup> Dawen Cai,<sup>1,4</sup> T. Lynne Blasius,<sup>1</sup> Gloria T. Jih,<sup>1</sup> Edgar Meyhofer,<sup>2,3,4</sup> Jacek Gaertig,<sup>5</sup> and Kristen J. Verhey<sup>1,3,\*</sup>

<sup>1</sup>Department of Cell and Developmental Biology

<sup>2</sup>Department of Mechanical Engineering

<sup>3</sup>Program in Cellular and Molecular Biology

<sup>4</sup>Program in Biophysics

University of Michigan

Ann Arbor, Michigan

<sup>5</sup>Department of Cellular Biology

University of Georgia

Athens, Georgia

## Summary

Long-distance intracellular delivery is driven by kinesin and dynein motor proteins that ferry cargoes along microtubule tracks [1, 2]. Current models postulate that directional trafficking is governed by known biophysical properties of these motors—kinesins generally move to the plus ends of microtubules in the cell periphery, whereas cytoplasmic dynein moves to the minus ends in the cell center. However, these models are insufficient to explain how polarized protein trafficking to subcellular domains is accomplished. We show that the kinesin-1 cargo protein JNK-interacting protein 1 (JIP1) is localized to only a subset of neurites in cultured neuronal cells. The mechanism of polarized trafficking appears to involve the preferential recognition of microtubules containing specific post-translational modifications (PTMs) by the kinesin-1 motor domain. Using a genetic approach to eliminate specific PTMs, we show that the loss of a single modification,  $\alpha$ -tubulin acetylation at Lys-40, influences the binding and motility of kinesin-1 in vitro. In addition, pharmacological treatments that increase microtubule acetylation cause a redirection of kinesin-1 transport of JIP1 to nearly all neurite tips in vivo. These results suggest that microtubule PTMs are important markers of distinct microtubule populations and that they act to control motor-protein trafficking.

## Results and Discussion

In most species, kinesin-1 (formerly conventional kinesin or Kif5) is a heterotetramer of two kinesin heavy chains (KHC) and two kinesin light chains (KLC). A direct interaction between the JIP proteins and KLC is required for kinesin-1-dependent transport of JIP1 to the tips of neurites in differentiating neuronal CAD cells [3]. Interestingly, only some neurites contain detectable JIP1 at their tips (Figure 1A; also Figure S1B in the Supplemental Data available online). Although JIP1 is delivered to the tips of neurites of all lengths (Figure 1B), in most

cases JIP1 signal is primarily present in the longest neurite of each cell (Figure 1C). Localization to only a subset of neurites can also be seen for a constitutively active form of the KHC motor both in differentiated CAD cells (Figure S2) and in primary hippocampal neurons ([4] and data not shown). These observations raise a key question: Why and how does kinesin-1 transport JIP1 to only a subset of neurites?

To analyze JIP1 transport by kinesin-1 in living cells, we genetically tagged JIP1 with the enhanced yellow fluorescent protein (EYFP). EYFP had no effect on JIP1 interactions with partner proteins and transport to the tips of neurites (Figure S1). Time-lapse confocal microscopy of differentiated CAD cells expressing EYFP-JIP1 showed continuous localization of EYFP-JIP1 to one neurite, whereas the other neurites lacked detectable EYFP-JIP1 (Figure 1D). To gain an understanding of the dynamics of JIP1 transport, we carried out fluorescence recovery after photobleaching (FRAP) experiments. The kinetics of EYFP-JIP1 recovery in bleached neurite tips indicates that the majority of EYFP-JIP1 molecules are turning over (Figures 1E–1G). These results indicate a continuous replenishment of JIP1 molecules by kinesin-1-dependent transport rather than a stationary population of JIP1 molecules that move with the growth cone.

What could be the mechanism by which kinesin-1 selectively delivers JIP cargo proteins to a subset of neurites? Previous studies have suggested that directed trafficking could be driven by “smart” motors that recognize environmental cues [5]. One potential biochemical cue is microtubule PTMs, such as deetyrosination, acetylation, and polyglutamylation, that occur after microtubule polymerization and accumulate on a subset of more stable microtubules in an age-dependent manner [6, 7]. Because at least some PTMs do not appear to change the intrinsic properties, such as stability, of microtubules, they have been postulated to “mark” subsets of microtubules and may thereby influence the binding of motors, microtubule-associated proteins (MAPs), or both [8]. This is supported by immunofluorescence staining of specific microtubule PTMs and the localization of active kinesin-1 motors and JIP1 cargoes in branched neurites (Figure S2).

To assess whether specific PTMs can directly influence the interaction of kinesin-1 with microtubules, we carried out microtubule binding assays by using ciliary axonemes purified from wild-type *Tetrahymena* and strains carrying  $\alpha$ - or  $\beta$ -tubulin mutations that eliminate sites of specific PTMs. As expected, both full-length Myc-KHC and a KHC dimeric motor [Myc-KHC(1–379)] bound to wild-type axonemes in the presence of AMPPNP (Figure 2A, lane 2). A partial loss of polymodifications (polyglycylation and polyglutamylolation) on the  $\beta$ -tubulin C-terminal tail (CTT) ( $\beta$ -EDDD<sub>440</sub> mutation [9]) had no effect on Myc-KHC binding, whereas a more severe loss of polymodifications at this site ( $\beta$ -EAAA mutation [9]) reduced Myc-KHC binding (Figure 2A, lanes 3

\*Correspondence: [kjverhey@umich.edu](mailto:kjverhey@umich.edu)

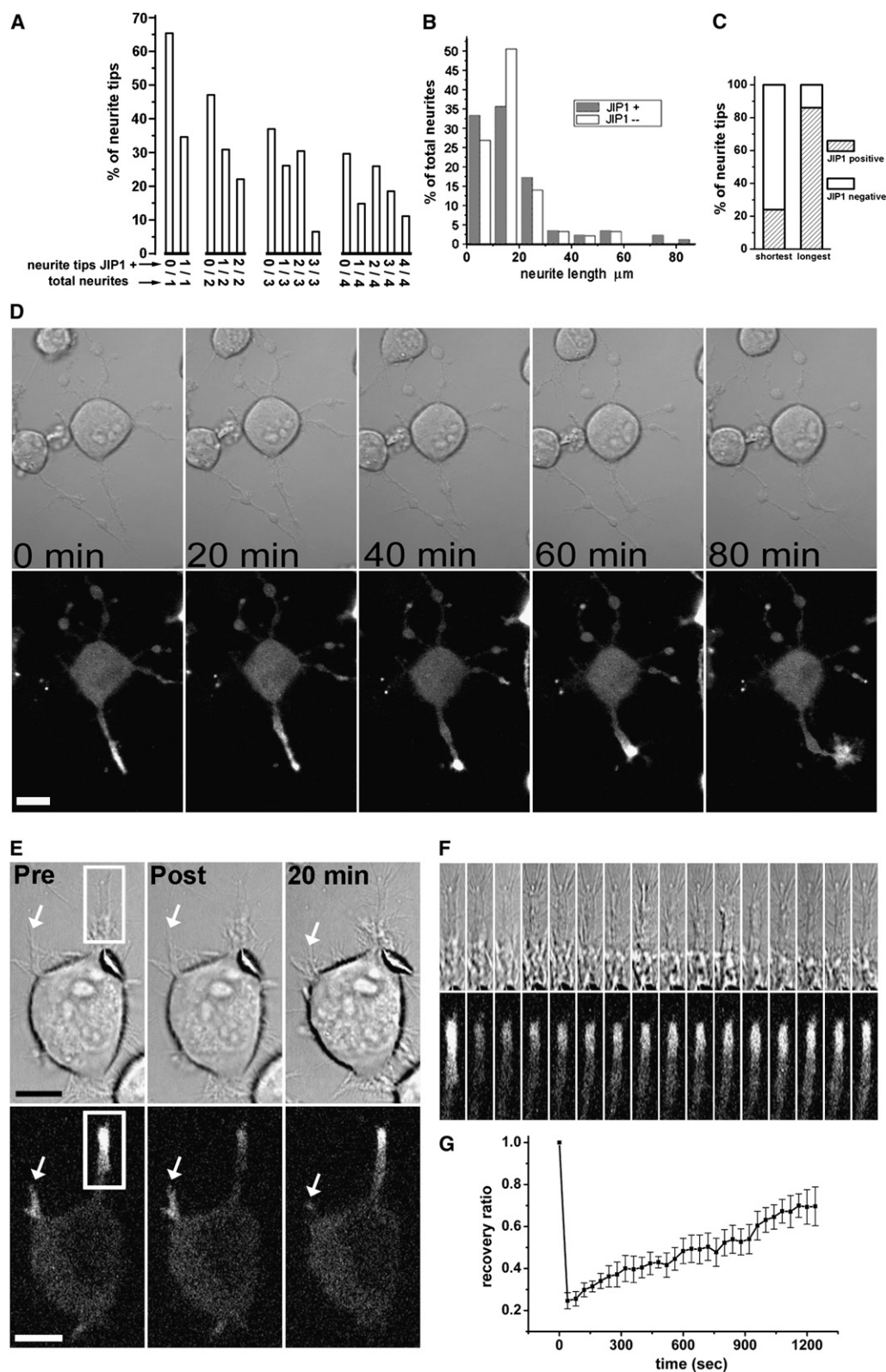
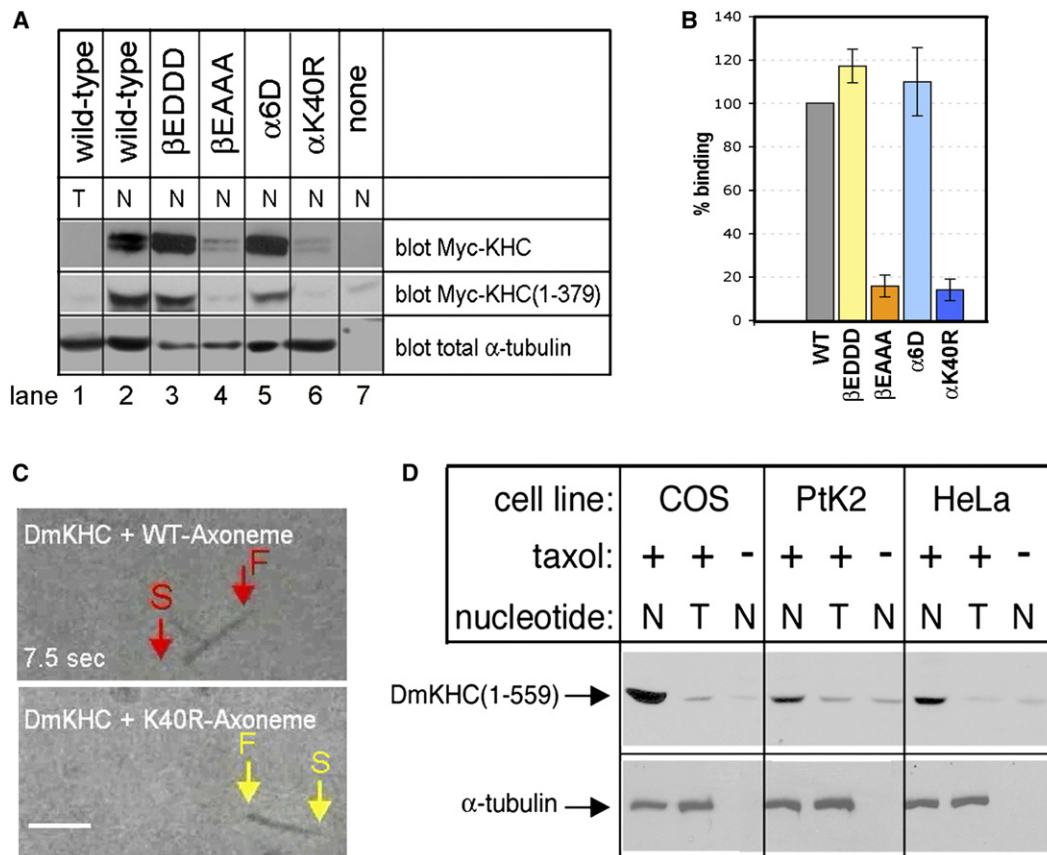


Figure 1. The JIP1 Cargo Protein Is Transported to a Subset of Neurites

(A–C) Differentiated CAD cells were immunostained for JIP1 and total  $\beta$ -tubulin. (A) The percent of neurites that have detectable JIP1 was determined for cells containing one to four neurites ( $n = 78, 68, 46$ , and  $27$  cells, respectively). (B) Neurite lengths were measured for JIP1-positive and JIP1-negative neurites. Data are expressed as the percent of neurites that fall in  $10 \mu\text{m}$  interval lengths for JIP1-positive (gray bars;  $n = 87$  neurites) and JIP1-negative (white bars;  $n = 93$  neurites). (C) The presence of JIP1 in the longest and shortest neurite was scored for individual cells ( $n = 49$ ) containing two or more neurites. Data are expressed as the percent of shortest and longest neurites that have detectable JIP1.



**Figure 2. Loss of Specific Microtubule PTMs Influences Kinesin-1 Binding and Motility**

(A) Microtubule binding assay. Ciliary axonemes isolated from wild-type or the indicated mutant *Tetrahymena* strains were incubated with Myc-KHC or Myc-KHC(1-379) in the presence of ATP (T) or AMPPNP (N). After centrifugation, the axoneme pellets were immunoblotted with antibodies to the Myc tag and  $\alpha$ -tubulin. Control experiments show that Myc-KHC and Myc-KHC(1-379) do not pellet in the presence of ATP (T) or in the absence of axonemes.

(B) Quantification of three binding experiments. Binding of Myc-KHC to mutant axonemes was normalized to wild-type axonemes (mean  $\pm$  standard error).

(C) In vitro gliding assay. Wild-type (top panel) and  $\alpha$ -K40R (bottom panel) *Tetrahymena* axonemes were used in gliding assays on a lawn of purified DmKHC. Arrows indicate the position of the leading end of axonemes at the start (S) and finish (F) of the assay. The image is the final frame of [Movie S1](#). The scale bar represents 3  $\mu$ m.

(D) Microtubule binding assay. Microtubules were polymerized (with taxol) or not (no taxol) from COS, PtK2, or HeLa cell tubulin and then incubated with recombinant DmKHC(1-559) in the presence of ATP (T) or AMPPNP (N). Microtubule pellets were immunoblotted with antibodies to KHC and  $\alpha$ -tubulin. The small amount of DmKHC(1-559) in the control lanes (+ATP and -taxol) is due to aggregation and pelleting of non-microtubule-bound DmKHC(1-559).

and 4). A complete loss of poly modifications on the  $\alpha$ -tubulin CTT ( $\alpha$ -6D mutation [J.G., unpublished data]) had no effect on Myc-KHC binding ([Figure 2A](#), lane 5). These results indicate that polyglycylation and/or polyglutamylation of the  $\beta$ -tubulin CTT, but not  $\alpha$ -tubulin CTT, influences kinesin-1-microtubule binding, consistent with kinesin-1 binding mainly to the  $\beta$ -tubulin subunit [10].

Elimination of  $\alpha$ -tubulin acetylation ( $\alpha$ -K40R charge-conserving mutation [11], [Figure S3A](#)) caused a significant loss of KHC binding ([Figure 2A](#), lane 6). This was

unexpected for several reasons. First, the kinesin binding site on the  $\beta$ -tubulin CTT was intact [10]. Second, acetylation of  $\alpha$ -tubulin at Lys-40 is thought to occur in the microtubule lumen [12]. Third, *Tetrahymena* bearing an  $\alpha$ -K40R mutation had no detectable mutant phenotype [11], suggesting that microtubule-based motors involved in ciliary transport and motility are unaffected by the mutation or loss of acetylation.

To determine whether microtubule acetylation affects kinesin-1 motility, we carried out in vitro gliding assays.

(D) Time course imaging of a differentiated CAD cell with EYFP-JIP1 localized to the tip of a neurite that grew and turned. Phase (top) and EYFP fluorescence (bottom) images collected at the indicated time points are shown.

(E) FRAP of an EYFP-JIP1-expressing neurite. Phase (top) and EYFP fluorescence (bottom) images were collected prebleach (pre), postbleach (post), and for the next  $\sim$ 20 min. EYFP-JIP1 fluorescence was lost from a retracting neurite that was not bleached (arrow) but recovered in the bleached neurite (white box). The scale bar represents 10  $\mu$ m.

(F) Stills (80 s intervals) from a movie of EYFP-JIP1 fluorescence recovery in the bleached neurite in (E).

(G) Quantification of EYFP-JIP1 fluorescence recovery in bleached neurites ( $n = 6$ ) of various lengths. Error bars are means  $\pm$  standard error.

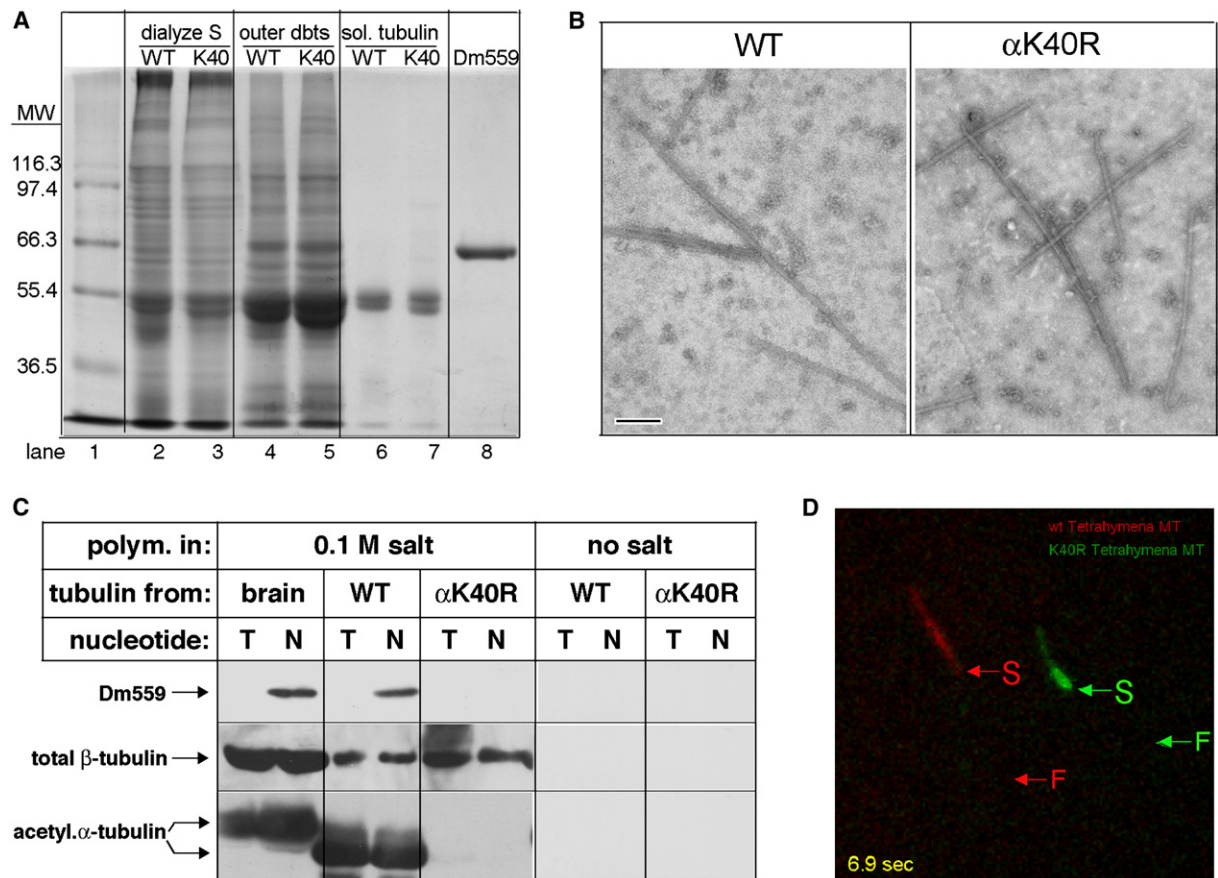


**Figure 3. Microtubule Acetylation Directly Affects the Binding and Motility of Kinesin-1**

(A) Coomassie-stained SDS-PAGE gel of the purification of soluble tubulin from wild-type (WT) or  $\alpha$ -K40R (K40) *Tetrahymena* axonemes. Lane 1, molecular-weight standards (in kD). Lanes 2 and 3, axonemal proteins released by dialysis. Lanes 4 and 5, outer doublet microtubules remaining after dialysis. Lanes 6 and 7, soluble tubulin released from outer doublets. Lane 8, recombinant DmKHC(1–559). Quantification of tubulin purity from three preparations is shown in Figure S4.

(B) Negative-stain electron microscopy shows normal morphology of microtubules repolymerized from purified wild-type or  $\alpha$ -K40R tubulin. The scale bar represents 500 nm.

(C) Microtubule binding assay. Bovine brain tubulin, wild-type *Tetrahymena* tubulin, and  $\alpha$ -K40R *Tetrahymena* tubulin repolymerized (0.1 M salt) or not (no salt) into microtubules were used in microtubule binding assays with recombinant DmKHC(1–559) in the presence of ATP (T) or AMPPNP (N). The microtubule pellets were immunoblotted for the presence of DmKHC(1–559), total  $\beta$ -tubulin, and acetylated  $\alpha$ -tubulin. Note that ciliate  $\alpha$ -tubulin runs more quickly on SDS-PAGE gels than mammalian  $\alpha$ -tubulin, whereas  $\beta$ -tubulins from ciliate and mammalian sources comigrate.

(D) In vitro gliding assays. Microtubules repolymerized from wild-type or  $\alpha$ -K40R *Tetrahymena* tubulin were labeled with 5- (and 6)-carboxy-*triamethylrhodamine succinimidyl ester* (TAMRA) and used in gliding assays with recombinant DmKHC(1–559). The image is an overlay of the final frame of gliding assays of TAMRA-WT (pseudocolored red) or TAMRA- $\alpha$ -K40R (pseudocolored green) microtubules recorded with the same length and time intervals. Arrows indicate the position of the leading end of microtubules at the start (S) and finish (F) of the assay.

Axonemes lacking  $\alpha$ -tubulin acetylation ( $\alpha$ -K40R mutation) moved at significantly ( $p < 0.001$ ) reduced speeds ( $0.47 \pm 0.05 \mu\text{m/s}$ ,  $n = 32$ ) on a lawn of purified *Drosophila* KHC in comparison to wild-type axonemes ( $0.61 \pm 0.03 \mu\text{m/s}$ ,  $n = 21$ ) (Figure 2C and Movie S1). The fact that more-dramatic effects are seen in the binding assay than in the gliding assay is likely due to the ability of individual weakly bound motors to cooperate at high densities in the gliding assay. Similar differences between assays that measure characteristics of a population of motors and those that measure properties of individual motors have been demonstrated for mutant kinesin-1 motors moving on wild-type microtubules [13, 14]. Taken together, these results indicate that acetylation of Lys-40 of  $\alpha$ -tubulin influences the enzymatic properties of kinesin-1.

To verify that it is the loss of acetylation, and not mutation of Lys-40, that influences kinesin-1, we utilized microtubules from cell lines containing known differences in PTM composition. COS and HeLa cells contain acetylated  $\alpha$ -tubulin, whereas PtK2 cells lack this modification (Figures S3B and S3C and [15]). In contrast, COS and PtK2 cells but not HeLa cells contain significant levels of deacetylated  $\alpha$ -tubulin (Figure S3B and [15]). Because these cell lines contain different levels of kinesin-1 protein (data not shown), recombinant dimeric KHC motor domain [DmKHC(1–559)] was used to ensure equal motor input. DmKHC(1–559) bound with higher affinity to microtubules polymerized from COS cells than to microtubules polymerized from PtK2 or HeLa cells (Figure 2D), suggesting that both acetylation and deacetylation influence kinesin-1 binding.



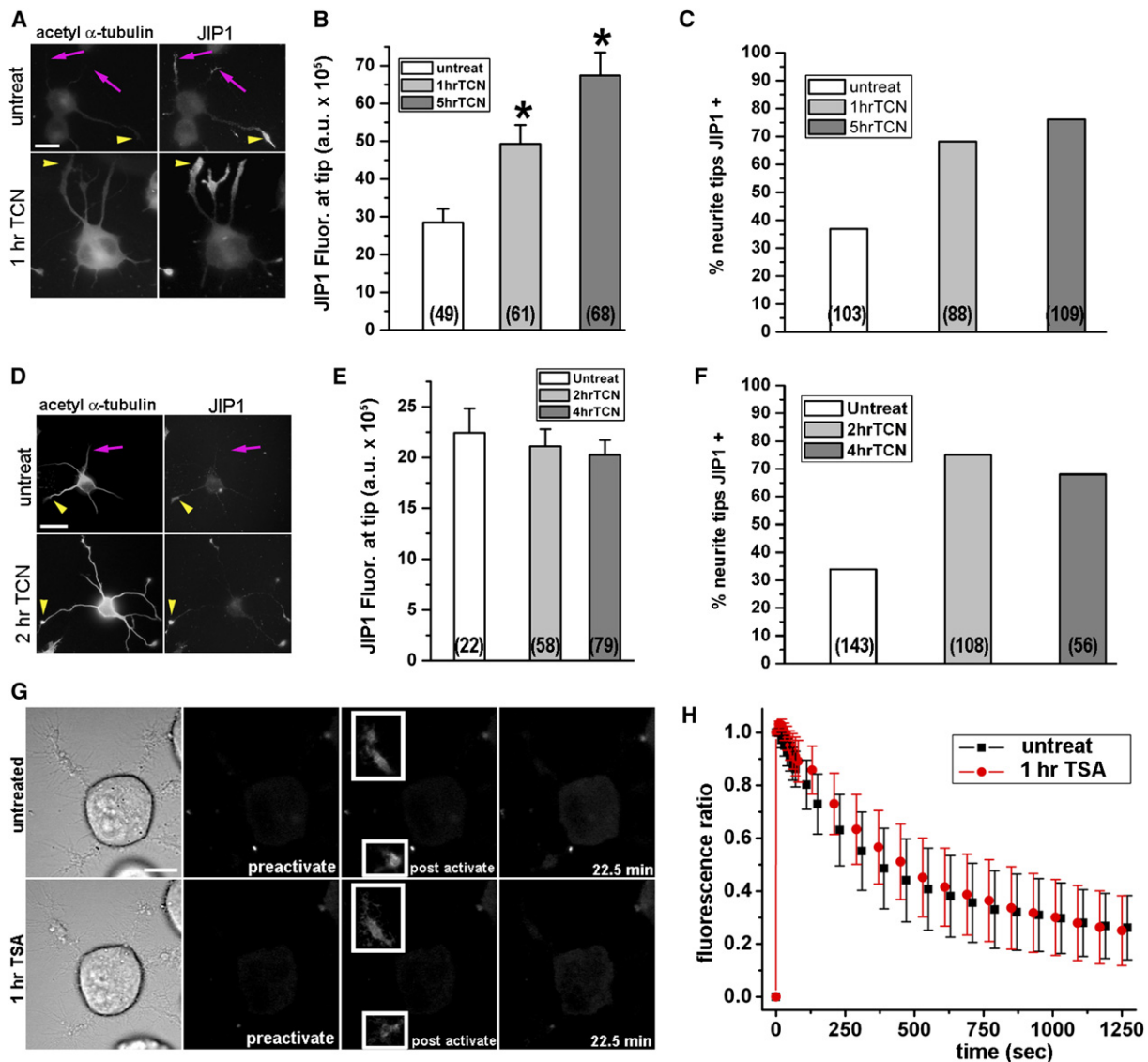


**Figure 4. Increased Microtubule Acetylation In Vivo Results in a Redirection of JIP1 Transport to Nearly All Neurite Tips**  
(A–F) Tubacin (TCN) treatment of differentiated CAD cells (A–C) or stage 2 primary hippocampal neurons (D–F). Untreated and TCN-treated cells were double labeled with antibodies to acetylated  $\alpha$ -tubulin and JIP1 (A and D) or total tubulin and JIP1 (Figure S5). Yellow arrowheads, JIP1-positive neurites; pink arrows, JIP1-negative neurites. Scale bars represent (A) 10  $\mu$ m and (B) 20  $\mu$ m. (B and E) Quantification of the amount of JIP1 immunoreactivity at the tips of neurites in untreated and TCN-treated cells for differentiated CAD cells (B) and primary hippocampal neurons (E). Values of n are in parentheses. Data are mean  $\pm$  standard error. An asterisk indicates  $p < 0.001$ . a.u. = arbitrary units. (C and F) Quantification of the percent of neurite tips that have JIP1 fluorescence in untreated and TCN-treated CAD cells (C) and primary hippocampal neurons (F). Values of n are in parentheses.  
(G and H) Tubacin causes no change in the loss of PAGFP-JIP1 from neurite tips.  
(G) Neurite tips in differentiated CAD cells expressing PAGFP-JIP1 were photoactivated (top panel, white boxes), and GFP images were collected for 22 min. The cells were treated with TSA for 1 hr, and then the same neurite tips were photoactivated (bottom panel, white boxes) and images were collected. The scale bar represents 10  $\mu$ m.  
(H) Quantification of the loss of PAGFP-JIP1 fluorescence in neurite tips (n = 5) before (black squares) and after (red circles) TSA treatment. Error bars are means  $\pm$  standard deviation.

The fact that the N-terminal region, including Lys-40, of expressed Ptk2 and HeLa  $\alpha$ -tubulin genes are identical (Figure S3D) indicates that it is acetylation and not mutation of  $\alpha$ -tubulin that influences kinesin-1 binding, although we cannot rule out the possibility that species-specific differences in the C-terminal half of  $\alpha$ -tubulin contribute. It is interesting, and perhaps surprising, that loss of a single PTM can affect kinesin-1 binding despite the continued presence of the other PTMs. In the

case of PTMs occurring on the  $\beta$ -tubulin CTT, this could be explained by CTT regulation of kinesin-1 mechanochemistry [8]. Because detirosination occurs on the CTT of  $\alpha$ -tubulin, a domain believed to be highly flexible [10], this PTM may also influence kinesin-1 binding to  $\beta$ -tubulin. How acetylation of  $\alpha$ -tubulin, located inside the microtubule, regulates kinesin-1 requires further study but may be due to subtle conformational changes across the tubulin dimer [16].

To test whether other factors (such as MAPs) present in the axonemes or COS cell lysates are required for the preferential binding of kinesin-1 to acetylated  $\alpha$ -tubulin, we purified tubulin protein from wild-type and  $\alpha$ -K40R *Tetrahymena* axonemes (Figure 3A; also Figure S4). Microtubules polymerized (Figure 3B) from  $\alpha$ -K40R *Tetrahymena* tubulin showed a significant decrease in binding to purified recombinant DmKHC(1–559) when they were compared to microtubules polymerized from bovine brain and wild-type *Tetrahymena* tubulin (Figure 3C). In gliding assays, microtubules polymerized from  $\alpha$ -K40R *Tetrahymena* tubulin showed a significant ( $p < 0.001$ ) decrease in velocity ( $0.38 \pm 0.02 \mu\text{m/s}$ ,  $n = 13$ ) on purified DmKHC(1–559) when they were compared to microtubules polymerized from wild-type *Tetrahymena* tubulin ( $0.46 \pm 0.03 \mu\text{m/s}$ ,  $n = 10$ ) (Figure 3D). Because purified components were used, these data indicate that acetylation of  $\alpha$ -tubulin directly influences the kinesin-1 motor domain.

To determine whether acetylation of  $\alpha$ -tubulin can influence kinesin-1 transport in vivo, we took advantage of pharmacological agents that increase the level of microtubule acetylation in cells. Treatment of differentiated CAD cells or stage 2 primary hippocampal neurons with trichostatin A (TSA), an inhibitor of class I and II histone deacetylases (HDACs) [17], caused a rapid increase in microtubule acetylation with a concomitant redirection of JIP1 transport to the tips of most neurites (data not shown). To confirm that these effects were due to alterations in microtubule acetylation, we treated cells with tubacin, a specific inhibitor of the  $\alpha$ -tubulin deacetylase HDAC6 [18]. Treatment of differentiated CAD cells or primary hippocampal neurons with tubacin resulted in increased levels of  $\alpha$ -tubulin acetylation despite there being no change in total tubulin content or  $\alpha$ -tubulin deacetylation (Figures 4A and 4D; also Figure S5). In individual neurites of primary hippocampal neurons double stained for acetylated  $\alpha$ -tubulin and total tubulin, the mean of the ratio of acetylated:total tubulin increased 2.5-fold upon tubacin treatment ( $n = 10$  each). Importantly, upon tubacin treatment, JIP1 no longer localized to a subset of neurites but rather accumulated at the tips of nearly all neurites (Figures 4A, 4C, 4D, and 4F). Tubacin treatment also caused an increase in the amount of endogenous JIP1 protein at neurite tips in CAD cells but not hippocampal neurons (Figures 4B and 4E), perhaps because of the higher levels of JIP1 protein in CAD cells (data not shown). Alternatively, acetylation may have slightly different effects in different cell types. The increased presence of JIP1 at neurite tips upon tubacin treatment cannot be explained by an increase in the width of the neurites (Figure S5E) or by a decrease in retrograde transport of JIP1 because the rate of loss of photoactivatable GFP-tagged JIP1 (PAGFP-JIP1) fluorescence from neurite tips was identical in untreated and treated CAD cells (Figures 4G and 4H). Taken together, these results indicate that microtubule PTMs, specifically  $\alpha$ -tubulin acetylation, cause a redirection of kinesin-1-dependent trafficking in vivo.

Polarized protein trafficking is critical for cell morphogenesis and function, but the mechanisms are not well understood [19–21]. In this study, we present an analysis of a cargo protein with polarized subcellular distribution as well as its known microtubule-based motor. We

provide results from several independent approaches that together provide strong evidence that microtubule PTMs influence the recruitment of kinesin-1 to specific microtubule tracks. One attractive possibility is that PTMs mark subsets of microtubules that lead to specific subcellular destinations. For example, acetylation may direct kinesin-1-based transport to growing neurites in developing neurons, to axons in mature cells, or both [4, 22, 23] and may also direct protein trafficking during formation and organization of the immune synapse in T cells [24], the migration of wound-edge fibroblasts [25, 26], and the preferential movement of mitochondria into growing axonal branch points [27]. Another possibility is that PTMs provide a biochemical signal that distinguishes cytoskeletal tracks most likely to extend all the way to the destination. Because the rate of microtubule growth in vivo ( $\sim 0.2 \mu\text{m/s}$  [28, 29]) is slower than the rate of vesicle transport in vivo (average velocity  $\sim 2.0 \mu\text{m/s}$  [30, 31]), it would be advantageous for the motor to travel selectively along the more stable cytoskeletal tracks marked by PTMs.

#### Supplemental Data

Supplemental Data include Experimental Procedures, five figures, and Movie S1 and are available online at <http://www.current-biology.com/cgi/content/full/16/21/2166/DC1/>.

#### Acknowledgments

We thank R. Mazitschek (Broad Institute) for the tubacin structural analog MAZ1370, W. Hancock (Pennsylvania State University) for expression plasmid of DmKHC(1–559), J. Lippincott-Schwartz (National Institutes of Health) for PAGFP plasmid, G. Gundersen (Columbia) for antibody to deetyrosinated tubulin, D. Gumucio and A. Diaz (University of Michigan) for help with RNA isolation, J. Duan and M. Gorovsky (University of Rochester) for the ATU1-6D plasmid, and K. Rogowski (University of Georgia) for providing the ATU1-6D strain of *Tetrahymena*. We are grateful to members of the Verhey lab for help and discussions, especially to J. Hammond for isolation of primary hippocampal neurons and to K. Griffin for RNA isolation. We thank T. Rapoport (Harvard) for critical reading of the manuscript. This work was supported in part by grants to K.J.V. (NIH GM070862) and J.G. (NSF MCB-0235826).

Received: May 1, 2006

Revised: September 6, 2006

Accepted: September 8, 2006

Published: November 6, 2006

#### References

- Hirokawa, N., and Takemura, R. (2005). Molecular motors and mechanisms of directional transport in neurons. *Nat. Rev. Neurosci.* 6, 201–214.
- Vallee, R.B., Williams, J.C., Varma, D., and Barnhart, L.E. (2004). Dynein: An ancient motor protein involved in multiple modes of transport. *J. Neurobiol.* 58, 189–200.
- Verhey, K.J., Meyer, D., Deehan, R., Blenis, J., Schnapp, B.J., Rapoport, T.A., and Margolis, B. (2001). Cargo of kinesin identified as JIP scaffolding proteins and associated signaling molecules. *J. Cell Biol.* 152, 959–970.
- Jacobson, C., Schnapp, B., and Banker, G.A. (2006). A change in the selective translocation of the Kinesin-1 motor domain marks the initial specification of the axon. *Neuron* 49, 797–804.
- Shah, J.V., and Goldstein, L.S. (2000). Does motor protein intelligence contribute to neuronal polarity? *Neuron* 26, 281–282.
- Rosenbaum, J. (2000). Cytoskeleton: functions for tubulin modifications at last. *Curr. Biol.* 10, R801–R803.
- Westermann, S., and Weber, K. (2003). Post-translational modifications regulate microtubule function. *Nat. Rev. Mol. Cell Biol.* 4, 938–947.

8. Lakamper, S., and Meyhofer, E. (2006). Back on track—On the role of the microtubule for kinesin motility and cellular function. *J. Muscle Res. Cell Motil.* 27, 161–171.
9. Redeker, V., Levilliers, N., Vinolo, E., Rossier, J., Jaillard, D., Burnette, D., Gaertig, J., and Bre, M.H. (2005). Mutations of tubulin glycylation sites reveal cross-talk between the C termini of alpha- and beta-tubulin and affect the ciliary matrix in *Tetrahymena*. *J. Biol. Chem.* 280, 596–606.
10. Marx, A., Muller, J., Mandelkow, E.M., Hoenger, A., and Mandelkow, E. (2005). Interaction of kinesin motors, microtubules, and MAPs. *J. Muscle Res. Cell Motil.* 27, 125–137.
11. Gaertig, J., Cruz, M.A., Bowen, J., Gu, L., Pennock, D.G., and Gorovsky, M.A. (1995). Acetylation of lysine 40 in alpha-tubulin is not essential in *Tetrahymena thermophila*. *J. Cell Biol.* 129, 1301–1310.
12. Nogales, E., Wolf, S.G., and Downing, K.H. (1998). Structure of the alpha beta tubulin dimer by electron crystallography. *Nature* 391, 199–203.
13. Friedman, D.S., and Vale, R.D. (1999). Single-molecule analysis of kinesin motility reveals regulation by the cargo-binding tail domain. *Nat. Cell Biol.* 1, 293–297.
14. Hackney, D.D., Stock, M.F., Moore, J., and Patterson, R.A. (2003). Modulation of kinesin half-site ADP release and kinetic processivity by a spacer between the head groups. *Biochemistry* 42, 12011–12018.
15. Bulinski, J.C., Richards, J.E., and Piperno, G. (1988). Posttranslational modifications of alpha tubulin: Detyrosination and acetylation differentiate populations of interphase microtubules in cultured cells. *J. Cell Biol.* 106, 1213–1220.
16. Krebs, A., Goldie, K.N., and Hoenger, A. (2004). Complex formation with kinesin motor domains affects the structure of microtubules. *J. Mol. Biol.* 335, 139–153.
17. Koeller, K.M., Haggarty, S.J., Perkins, B.D., Leykin, I., Wong, J.C., Kao, M.C., and Schreiber, S.L. (2003). Chemical genetic modifier screens: Small molecule trichostatin suppressors as probes of intracellular histone and tubulin acetylation. *Chem. Biol.* 10, 397–410.
18. Haggarty, S.J., Koeller, K.M., Wong, J.C., Grozinger, C.M., and Schreiber, S.L. (2003). Domain-selective small-molecule inhibitor of histone deacetylase 6 (HDAC6)-mediated tubulin deacetylation. *Proc. Natl. Acad. Sci. USA* 100, 4389–4394.
19. Lecuit, T., and Pilot, F. (2003). Developmental control of cell morphogenesis: A focus on membrane growth. *Nat. Cell Biol.* 5, 103–108.
20. Rodriguez-Boulant, E., Kreitzer, G., and Musch, A. (2005). Organization of vesicular trafficking in epithelia. *Nat. Rev. Mol. Cell Biol.* 6, 233–247.
21. Horton, A.C., and Ehlers, M.D. (2003). Neuronal polarity and trafficking. *Neuron* 40, 277–295.
22. Letourneau, P.C., and Wire, J.P. (1995). Three-dimensional organization of stable microtubules and the Golgi apparatus in the somata of developing chick sensory neurons. *J. Neurocytol.* 24, 207–223.
23. Nakata, T., and Hirokawa, N. (2003). Microtubules provide directional cues for polarized axonal transport through interaction with kinesin motor head. *J. Cell Biol.* 162, 1045–1055.
24. Serrador, J.M., Cabrero, J.R., Sancho, D., Mittelbrunn, M., Urzainqui, A., and Sanchez-Madrid, F. (2004). HDAC6 deacetylase activity links the tubulin cytoskeleton with immune synapse organization. *Immunity* 20, 417–428.
25. Hubbert, C., Guardiola, A., Shao, R., Kawaguchi, Y., Ito, A., Nixon, A., Yoshida, M., Wang, X.F., and Yao, T.P. (2002). HDAC6 is a microtubule-associated deacetylase. *Nature* 417, 455–458.
26. Palazzo, A., Ackerman, B., and Gundersen, G.G. (2003). Cell biology: Tubulin acetylation and cell motility. *Nature* 421, 230.
27. Ruthel, G., and Hollenbeck, P.J. (2003). Response of mitochondrial traffic to axon determination and differential branch growth. *J. Neurosci.* 23, 8618–8624.
28. Rusan, N.M., Tulu, U.S., Fagerstrom, C., and Wadsworth, P. (2002). Reorganization of the microtubule array in prophase/prometaphase requires cytoplasmic dynein-dependent microtubule transport. *J. Cell Biol.* 158, 997–1003.
29. Salaycik, K.J., Fagerstrom, C.J., Murthy, K., Tulu, U.S., and Wadsworth, P. (2005). Quantification of microtubule nucleation, growth and dynamics in wound-edge cells. *J. Cell Sci.* 118, 4113–4122.
30. Hill, D.B., Plaza, M.J., Bonin, K., and Holzwarth, G. (2004). Fast vesicle transport in PC12 neurites: velocities and forces. *Eur. Biophys. J.* 33, 623–632.
31. Lippincott-Schwartz, J. (2004). Dynamics of secretory membrane trafficking. *Ann. N Y Acad. Sci.* 1038, 115–124.